Chalcogenide Letters Vol. 8, No. 7, July 2011, p. 419 - 426

INFLUENCES OF THERMAL ANNEALING ON THE STUCTURAL, OPTICAL AND ELECTRICAL PROPERTIES OF NANOSTRUCTURED CADMIUM SULPHIDE THIN FILMS

G. BAKIYARAJ[a], N. GOPALAKRISHNAN[b] and R. DHANASEKARAN[a*]
[a]*Crystal Growth Centre, Anna University , Chennai - 600025, India.*
[b]*Department of Physics, National Institute of Technology, Tirchirappalli – 620015, India.*

Cadmium sulphide (CdS) nano-crystallites thin films have been grown on an amorphous glass substrate in a polymer (polyvinyl alcohol) matrix solution using chemical bath deposition process. The samples annealed in air for 1 h at various temperatures and they are characterized for their structural, optical and electrical properties. It was confirmed from X-ray diffraction analysis that all the films exhibited a polycrystalline nature and hexagonal structure with (002) as the preferred orientation. The structural parameters such as particle size, strain, dislocation density and number of crystallites per unit area were calculated. The surface morphology of CdS thin films was analyzed by scanning electron microscope. Optical band gap studies indicated that the band gap of as-deposited sample has blue shift with respect to the corresponding value for the bulk CdS material. The band gap of the annealed samples decreased with the increase in annealing temperature i.e., a decrease in band gap value from 3.5 eV to 2.9 eV. Resistivity, Hall mobility, and carrier density were evaluated by Hall effect measurement at room temperature.

(Received June 14, 2011; Accepted July 13, 2011)

Keywords: Nanostructured materials, Structural properties, Optical properties, Electrical properties

1. Introduction

Current research on the study of nanometer-scale materials (usually 1-100 nm, also called nanomaterials) generates intense interest because it exhibits new or enhanced size-dependent properties compared with the larger size particles of the same material [1]. In tandem with surface-area effects, quantum effects can begin to dominate the properties of matter as size is reduced to the nanoscale. These can affect the optical, electrical and structural properties of materials [2]. In principle; the properties of semiconductor materials can be tuned by varying their size and shapes. Thus, the preparation of semiconductor nanostructured materials of controlled size and shape are of special interest. CdS belonging to the II-VI group is one of the promising materials for use in photoelectric conversion in solar cell [3], thin film transistor (TFT) [4], nonlinear optics [5], semiconductor laser [6] and flat panel display [7].

In the past few decades, several techniques were used for the preparation of nanostructured CdS thin film like molecular beam epitaxy (MBE) [8], chemical vapor deposition [9], electro deposition [10], spray pyrolyis [11] and chemical bath deposition [12]. CBD is a simple, low temperature, inexpensive and large-area deposition technique and it does not limit the choice of the substrate material. The low temperature deposition avoids oxidation and corrosion of the metallic substrate. The CBD grown CdS nanostructure thin films are strongly dependent on the preparation conditions such as temperature, stirring time, relative concentration and type of reactants [13-15]. In some of the solution-phase deposition methods, controlling size, shape and

*Corresponding author: rdhanasekaran@annauniv.edu, rdcgc@yahoo.com

dispersion of nanostructures have been achieved by using the templates (porous alumia [16], mesoporous silica [17]), zeolite [18], and in polymer matrix [19]. The use of polymers is a prominent method for the synthesis of semiconductor nanoparticles. The reason is that the polymer matrices provide for solubility, and control of the

growth and morphology of the nanoparticles. The PVA (polyvinyl alcohol), which is a water-

soluble polymer, has an excellent effect on the growth of CdS nanocrystals [20]. The role of thermal annealing (or) doping ion process is very important in achieving high performance devices. Therefore, studies of annealing effect on the surface morphology, the structural, optical and electrical properties are important in enhancing device efficiency [21-23]. Ghosh et al reported a field-emission properties of nanocrystalline CdS thin films grown by chemical bath deposition (CBD) within the pores of polyvinyl alcohol (PVA) on Si and glass substrates [24]. An aqueous solution system for growing hydrophobic honeycomb network of CdS thin film was investigated via PVA assisted route [25]. In this article, it is reported that a systematic study of the effect of annealing on morphological, structure, optical and electrical properties of CBD grown nanostructured CdS thin films in PVA matrix solution.

2. Experimental

2.1. Substrate cleaning

The substrate cleaning is very important in the deposition of thin films. Commercially available glass slides with a size of 75 mm x 25 mm x 1.35 mm were cleaned by a mild soap solution. The glass slides were degreased with acetone, etched with 5% of HCl for 30 min., ultrasonically cleaned by de-ionized water and finally dried in the air.

2.2. CdS thin film deposition

Cadmium sulfide thin films were deposited on glass substrate by chemical deposition method using analytical grade polyvinyl alcohol, cadmium chloride, ammonium chloride, 25% liquor ammonia and thiourea. To obtain deposition, 2 g of PVA $(-C_2H_4O)_n$ (MW = 1750) were dissolved in 250 ml of double distilled water and this mixture was kept at constant stirring at a constant temperature (75 °C) until a viscous transparent solution was obtained. Subsequently the temperature of the PVA solution was reduced to 40 °C. A mixture of NH_4Cl and $CdCl_2$ dissolved in NH_4OH containing 25% NH_3 (density of 0.91 g/m^3) was added to the PVA solution, again heating and stirring was continued. After complete desolation, thiourea dissolved in 30 ml distilled water, was added to the above solution. After the required temperature of 75 °C is reached, a cleaned glass substrate was mounted vertically into the above solution with the help of substrate holder. After deposition of 20 min, the substrate was taken out, thoroughly washed and rinsed with double distilled water and dried in the air.

2.3. Annealing of CdS thin films

The postdeposition thermal annealing processes were performed in an open horizontal tubular furnace in the temperature range of 300, 400, 500 °C for a fixed time of 1 hour. The samples were introduced into the furnace and removed at the annealing temperature to ensure a rapid heating and cooling of the samples.

2.4. Characterization techniques

The crystalline structure of the films was studied by x-ray diffraction measurements obtained with a Rigaku X-Ray Diffractometer (XRD) in the 2θ range of 10°- 80° using CuK_α radiation of wavelength λ=1.5406Å. X -ray tube was operated at 40 kV (Voltage) and 30 mA (current) with scanning speed of 0.5°/min. The surface morphology of the films was studied using

a LEO 440 STEROCAN (LEICA) scanning electron microscope. Optical absorption spectra of films were recorded with a SHIMAZDU 1700 UV-Vis spectrometer over wavelength range from 200 to 800 nm. Resistivity, Hall mobility, and carrier density were evaluated by Hall effect measurement at room temperature in a van der Pauw four-point probe configuration, using silver paste as contact, in an automated Hall effect system equipment (ECOPIA HMS – 3000). The thickness of the films was measured using filmetrics thickness measurement system.

3. Results and discussion

3.1. X-ray Diffraction Study

The diffraction spectra for as-deposited and postdeposition thermal annealed samples are shown in Fig. 1.The figure shows that the diffraction peaks appear weak by a low grain size and/or a thin sample presenting a broad noisy background [26]. The XRD pattern of the as-deposited sample exhibits only sharp diffraction peaks at $2\theta = 26.5^{\circ}$ which could be produced either by (002) the hexagonal (JCPDS- 89-2944) or (111) the cubic (JCPDS- 89-0440). It is quite difficult to differentiate the cubic from the hexagonal structure because the cubic (111) and the hexagonal (002) lines coincide with in 1% [27]. Many workers reported that the CdS film grown by CBD with ammonia based recipes have a high preferred orientation along with the (002) hexagonal structure [28-30]. There was no further analysis carried out to solve this uncertainty. When the annealing temperature is increased, the (002) peak intensity gradually increases and FWHM decreases indicating an improvement in the crystallinity of the film as shown in table 1. However, we remark that, at a high annealing temperature (500 °C), the hexagonal-phase presence can be clearly observed from the appearance of other one well defined characteristic peak at $2\theta = 28.1$ for (101) of hexagonal structure. Since this seems to be more stable structure, it is preferable to solar cell applications [31]. The average size (τ) of CdS clusters can be estimated using the Scherrer equation [32].

$$\tau = K\lambda / \beta \cos\theta \quad (1)$$

where K is the shape factor of a value of 0.9, λ is the wavelength of the incident X-ray, β is FWHM in radians and θ is the Bragg's angle. When the (002) diffraction peak in Fig. 1 is chosen for the calculation, it has been observed that the average crystallites size of the deposited film increases from 6 to 14 nm when the film is annealed at 500 °C.

The micro strain (ε), dislocation density (δ) and number of crystallites per unit area (N) [33-35] have been calculated using the following relations and their values are given in the table 1.

$$\text{Micro strain } (\varepsilon) = \beta \cos\theta / 4 \quad (2)$$

$$\text{Dislocation density } (\delta) = 1/\tau^2 \quad (3)$$

$$\text{Number of crystallites per unit area } (N) = t/\tau^3 \quad (4)$$

where t is the thickness of the film. It is interesting to note that the annealing temperature increases the dislocation density and decreases the strain in the films.

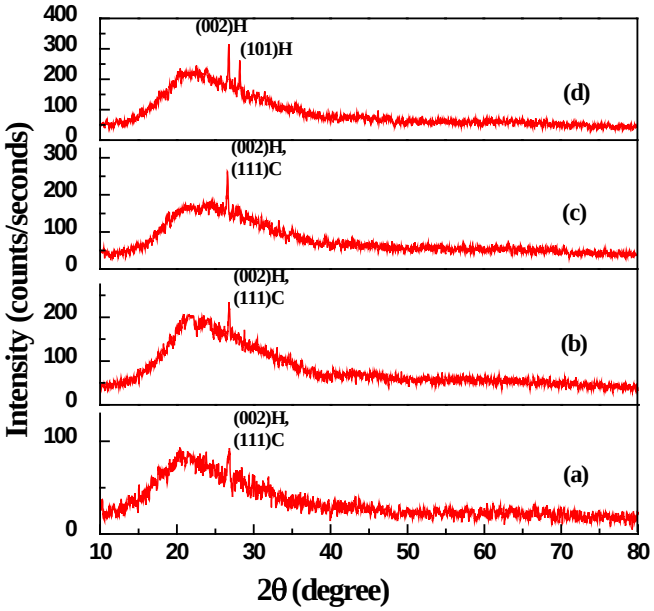

Fig. 1. XRD spectra of CdS thin films (a) as-deposited (at 75 °C), (b) annealed at 300 °C, (c) annealed at 400 °C, (d) annealed at 500 °C

Table. 1. Structural parameters of CdS thin film samples before and after annealing treatment

Sample	FWHM ($x10^{-3}$(rad.))	Grain size (nm)	Dislocation density (10^{15} lines/m^2)	Number of grains/unit area (10^{16} m^{-2})	Strain (10^{-4})
As-deposited	21.980	6.48	24.414	42.340	53.462
Annealed at 300 °C	16.048	8.87	12.913	17.168	39.039
Annealed at 400 °C	12.036	11.51	7.181	7.120	30.091
Annealed at 500 °C	9.420	14.71	4.627	3.683	23.550

3.2 Morphology of CdS thin film

The scanning electron microscope (SEM) images of as-deposited samples are shown in Fig. 2 (a)**.** From the figure, it is observed that the grains are in regular size and shape and the films are not well covered on the glass substrate. The grain sizes can be controlled by using parameters such as concentration of ingredients in the solution, bath temperature and time of the deposition. During the growth of the film, the PVA molecules acting as a stabilizer of CdS crystals being formed, interrupting their growth at the stage of nanoparticle formation. This means that the PVA reduces the agglomeration of nanoparticle on the substrate. This has resulted in a noticeable discontinuity between the grains and the voids in the layers of as-deposited sample. The crystallite size obtained from XRD Scherrer's equation (~6nm) was lower than the observed value from SEM. This may be due to the average size of crystallites obtained from XRD whereas from SEM, the obtained sizes were from the surface of the grains. Özsan et al reported transmission electron microscopy measurements that these CdS grain aggregates are composed by much smaller crystallites with an average size very similar to that determined from XRD measurement [36]. Fig

2 (b) show the SEM images of the films annealed at 500 °C respectively. From this figure it is observed that the increase of annealing temperature, grain size of CdS film becomes larger.

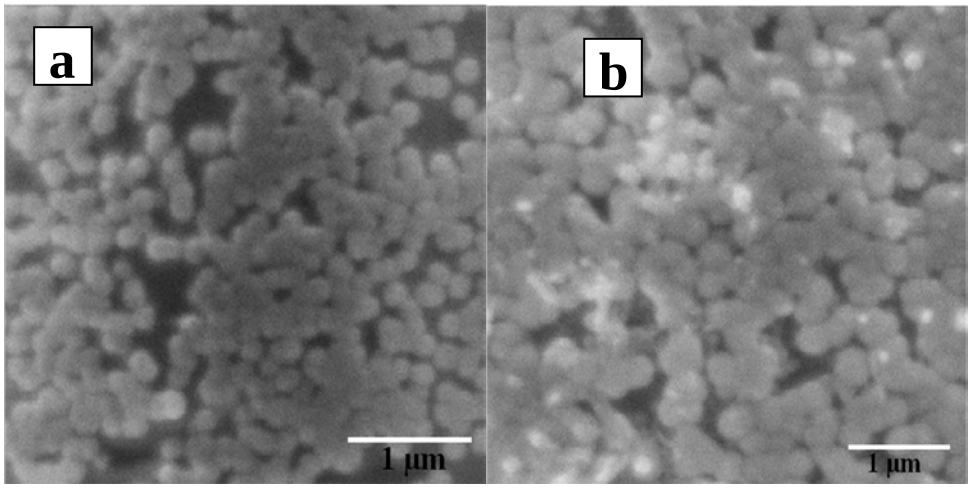

Fig. 2. SEM images of CdS thin films (a) as-deposited (at 75 °C), (b) annealed at 500 °C

3.3 Optical properties

UV-visible absorption spectra of as-deposited samples and annealed samples are shown in Fig. 3. The fundamental absorption, which corresponds to electron excitation from the valance to conduction bands, can be used to determine the nature and value of the optical band gap. The optical band gap (E_g) has been calculated using Tauc's formula [37],

$$\alpha = (A/h\nu)\,(h\nu - E_g)^n \tag{5}$$

where α is the absorption coefficient, (hν) is the incident photon energy, A is a constant, and the exponent n assumes the values ½, 2, 3/2 and 3 for allowed direct, allowed indirect, forbidden direct and forbidden indirect transitions, respectively. As CdS is a direct band gap material, n = ½ for the allowed transition

$$\alpha\, h\nu = A(h\nu - E_g)^{1/2} \tag{6}$$

The band gap has been calculated by extrapolating the linear region of the plots $(\alpha h\nu)^2$ vs hν on the energy axis, as shown in Fig. 4. Which are higher than that of the bulk value of CdS (2.42 eV at 300 K). The decrease of band gap (red shift) with the increase in annealing temperature is observed as shown in Fig. 5. It was clear that the band gap is decreased due to an increase of the cluster size or grain size and this is known as the quantum size effect. The enhancement of band gap is attributed to the quantum size effect of these small crystallites, although the diameters of the nanoparticles are quite larger than the excitonic Bohr radius (~3.5 nm) of CdS [19,38,39]. It may be noted that, when the as-deposited sample was annealed at 500 °C, the band gap decreases from 3.5 to 2.9 eV due to the increase of crystallite size. The crystallite size increases at a higher annealing temperature, as predicted by the thermodynamical behavior of growth of colloidal nanoparticles.

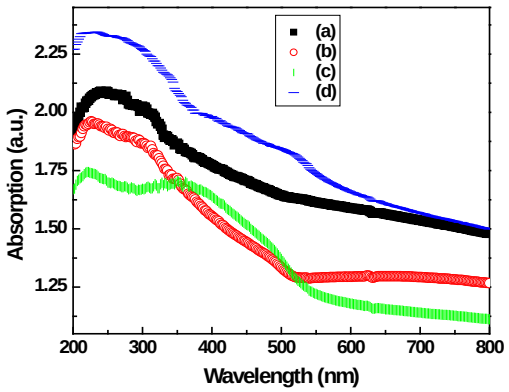

Fig. 3. UV-VIS absorption spectra of CdS thin films (a) as-deposited (b) annealed at 300 °C, (c) annealed at 400 °C, (d) annealed at 500 °C

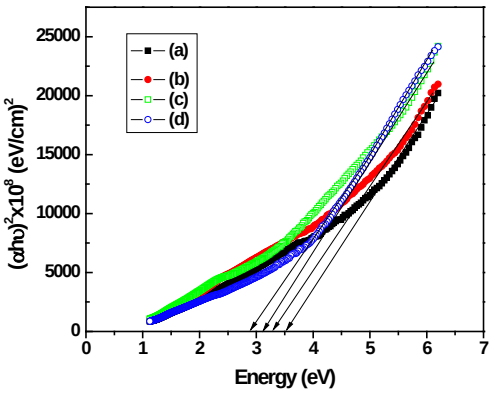

Fig. 4. A plots of $(\alpha\hbar\nu)^2$ vs. $\hbar\nu$ of CdS thin films (a) as-deposited (b) annealed at 300 °C, (c) annealed at 400 °C, (d) annealed at 500 °C

3.4 Electrical properties

The resistivity ρ, Hall mobility μ_H, and carrier concentration n of as-deposited and annealed samples were determined using Hall effect measurement and the values are shown in Table 2. The electrical resistivity at room temperature was in the order of 10^5 Ω cm for as-deposited CdS thin films which was decreased to 10^3 Ω cm after annealing at the temperature of 500 °C. The electrical resistivity of as-deposited CdS film is greater when it is compared to the values reported in literature [40,41]. It may be due to the nanocrystalline nature of thin film, crystallite boundary discontinuities, presence of surface states and small thickness of the film. It is evident that the value of electrical resistivity decreases with the increase in annealing temperature which confirms the semiconducting behavior of CdS film. The decrease in electrical resistivity with the increase in annealing temperature is due to the improvement in crystallite and/or grain size, decrease in defects and grain boundary discontinuities. The as-deposited film has a carrier concentration (C.C) of about 7.138 x 10^{11} cm^{-3}. The C.C value increases with the increase of annealing temperature and it reaches a value of about 1.169 x 10^{13} cm^{-3} at annealing temperature of 500 °C. The negative sign in Hall coefficient and C.C indicates that the as-deposited and annealed CdS thin films have n-type conductivity. The change in the conductivity due to annealing is shown in table 2. All the results shown above illustrate that the annealing treatment has a strong influence on the electrical properties of CdS thin films and that it is a good technique to improve the electrical conductivity of the as-deposited CdS thin films.

Table. 2. Electrical properties of CdS thin film before and after annealing

Sample	Resistivity (Ω cm)	Mobility (cm^2/Vs)	Carrier concentration (cm^{-3})	Conductivity $(\Omega\ cm)^{-1}$
As-deposited	1.473 x10^5	5.936 x10^1	-7.138 x10^{11}	6.787 x10^{-6}
Annealed at 300 °C	7.440 x10^3	9.872 x10^1	-8.499 x10^{12}	1.344 x10^{-4}
Annealed at 400 °C	3.079 x10^3	2.408 x10^1	-8.418 x10^{13}	3.248 x10^{-4}
Annealed at 500 °C	1.858 x10^3	2.878 x10^2	-1.169 x10^{13}	5.383 x10^{-4}

4.Conclusion

CBD is a simple technique to prepare CdS nanocrystalline thin films at low temperature. These CdS deposits are uniformly distributed particles, each consisting of many smaller nanocrystllites (~6 nm). The nanostructure of CdS was confirmed by XRD. When the sample is annealed at 500 ˚C, it has (101) additional peak at 28.1˚ which confirms the single phase of hexagonal structure. The surface morphology and grain size of CdS films are found to vary with the thermal annealing temperature. With the increase in annealing temperature, the grain size becomes larger and it becomes denser. From optical absorption measurements, it is found that the optical band gap reduces from 3.5 eV to 2.9 eV, i.e. optical band gap of semiconductor nanocrystals can be tuned as desired by using the annealing temperature. Electrical measurement confirms that the resistivity decreases to the order of 10^3 Ω cm and increase in electrical conductivity due to annealing.

Acknowledgements

This project is (UFUP 41323) supported by the Inter University Accelerator Centre (IUAC), New Delhi, India. The authors wish to acknowledge Mr.K.T.Tamilmani, Assistant Professor and Head, Department of English, Nehru Memorial College, Puthanampatti for having taken efforts to prune the sentences and refine the language.

Reference

[1] P. Zhang, P.S. Kim, T.K. Sham, J. Appl. Phys. **91**, 6038-6043 (2002).
[2] Guozhong Cao, Nanostructures & Nanomaterials, first edition, Imperial College Press, London (2004).
[3] R.S. Singh, V.K. Rangari, S. Sanagapalli, V. Jayaraman, S. Mahendra, V.P. Singh, Sol. Energy Mater. Sol. Cells **82**, 315-330 (2004).
[4] F.Y. Gan, I. Shih, IEEE Trans. Electron. Dev. **49**, 15-18 (2002).
[5] M.H. Majles Ara, Z. Dehghani, E. Saievar Iranized, Int. J. Nanotecnol. **6**, 1006-1014 (2009).
[6] X. Duan, Y. Huang, R. Agarwal, C.M. Lieber, Nature (London) **421**, 241-245 (2003).
[7] S. Schmitt-Rink, D.S. Chemla, D.A.B. Miller, Adv. Phys. **38**, 89-188 (1989).
[8] Boon K. Teo, X. H. Sun, Chem. Rev. **107**, 1454-1532 (2007).
[9] R M Ma, X L Wei, L Dai, H B Huo, G G Qin, Nanotechnology, **18**, 205605 (2007).
[10] J.I. Ceserano, E. Burch, G.P. Lopez, X. Xu, Thin Solid Films, **305**, 95-102 (1997).
[11] M.C. Baykul, A. Balciolu, Microelctron. Eng. **51-52**, 703-713 (2000).
[12] Xin Song, Ying-Song Fu, Yang Xie, Jun-Guo Song, Hong-Li Wang, Jing Sun, Xi-Wen Du, Semicond. Sci. Technol. **25**, 045031 (2010).
[13] R.S. Mane, C.D. Lokhande, Mater. Chem. Phys. **65**, 1-31 (2000).
[14] C.H. Henry, J. Appl. Phys. **51**, 4494-4500 (1980).
[15] S.N. Sahu, J Mat Sci: Mater Electron **6**, 43 (1995).
[16] S.P. Mondal, K. Das, A. Dhar, S.K. Ray, Nanotechnology **18**, 095606 (2007).
[17] Cheng-Yu Lai, Brian G. Trewyn, Dusan M. Jeftinija, Ksenija Jeftinija, Shu Xu, Srdija Jeftinija, Victor S.-Y. Lin, J. Am. Chem. Soc. **125**, 4451-4459 (2003).
[18] Ying Wang and Norman Herron, J. Phys.Chem. **92** (1988) 4988-4994.
[19] S.P. Mondal, H. Mullick, T. Lavanya, A. Dhar, S.K. Ray, S.K. Lahiri, J. Appl. Phys. **102**, 064305 (2007).
[20] Hongmei Wang, Pengfei Fang, Zhe Chen, Shaojie Wang, Appl. Surf. Sci. **253**, 8495-8499 (2007).
[21] W.J. Danaher, L.E. Lyons, G.C. Morris, Sol. Energy Mater. **12**, 137 (1985).
[22] H. Oumous, H. Hadiri, Thin Solid Films, **386**, 87-90 (2001).
[23] Hani Khallaf, Guangyu Chai, Oleg Lupan, Lee Chow, S. Park, Alfons Schulte, Appl. Surf. Sci. **255**, 4129-4134 (2009).
[24] P.K. Ghosh, S. Jana, U.N. Maity, K.K. Chattopadhyay, Physica E, **35**, 178–182 (2006).

[25] D.S. Dhawale, D.P. Dubal, R.J. Deokate, T.P. Gujar, Y.K. Sun, C.D. Lokhande, J. Alloys Compd. **503**, 422-425 (2010).
[26] Cortes, H. Gomez, R. E. Marotti, G. Riveros, E. A. Dalchiele, Sol.Energy Mater. Sol. Cells **82**, 21-34 (2004).
[27] O. Zelaya-angel, L. Hernandez, O de Melo, J J Alvarado-Gil, R Lozada-Morales, C Falcony, H Vargas, R Ramirez-Bon, Vacuum, **46**, 1083-1085 (1995).
[28] Kodigala Subba Ramaiah, R.D. Pilkington, A.E. Hill, R.D. Tomlinson, A.K. Bhatnagar, Mater. Chem. Phys. **68**, 22-30 (2001).
[29] A.I. Oliva, O. Solis-Canto, R. Castro-Rodriguez, P. Quintana, Thin Solid Films, **391**, 28-35 (2001).
[30] R. Ramirez-Bon, N.C. Sandoval-Inda, F.J. Espinoza-Beltrán, M. Sotelo-Lerma, O. Zelaya-Angel, C. Falcony, J. Phys.: Condens. Matter. **9**, 10051-10058 (1997).
[31] I. Kaur, D. K. Pandya, K.L. Chopra, J. Electrochem. Soc. **127**, 943-948 (1980).
[32] B.D. Cullity, Elements of X-ray Diffraction, second edition, Addison-Wesley (1978).
[33] V.Bilgin, S. Kose, F. Atay, I. Akyur, Mater. Chem. Phys. **94**, 103-108 (2005).
[34] J.B. Seon, S. Lee, J.M. Kim, H.D. Jeong, Chem. Mater. **21** (2009) 604-611.
[35] M.B. Ortuño López, J.J . Valenzuela-Jáuregui, M. Sotelo-Lerma, A. Mendoza-Galván, R. Ramirez-Bon, Thin Solid Films **429**, 34-39 (2003).
[36] M.E. Özsan, D.R. Johnson, M. Sadeghi, D. Sivapathasundaram, G. Goodlet, M.J. Furlong, L.M. Peter, A.A. Shingleton, J. Mat. Sci.: Mat. Elect. **7**, 119-125 (1996).
[37] J. Tauc, R. Grigorovici, A. Vancu, Phys. Stat. Solidi **15**, 627 (1966).
[38] R. Maity, K.K. Chattopadhyay, J Nanopart Res. **8** (2006) 125-130.
[39] A.P. Alivisatos, J. Phys. Chem. **100**, 13226-13239 (1996).
[40] J. Hiie, T. Dedova, V. Valdna, K. Muska, Thin Solid Films, **511-512**, 443-447 (2006).
[41] S.A. Tomás, O. Vigil, J.J.Alvarado-Gil, R. Lozada-Morales, O. Zelaya-Angel, H. Vargas, A. Ferreira da Silva, J. Appl. Phys. **78**, 2204-2207 (1995).